Effect of Transformation Temperature on the Ferrite–Bainite Microstructures, Mechanical Properties and the Deformation Behavior in a Hot-Rolled Dual Phase Steel

Bo Jiang[1] · Xuewen Hu[1,2] · Leyu Zhou[3] · Haibo Wang[1] · Yazheng Liu[1] · Fugang Gou[4]

Abstract

The ferrite–bainite microstructures and mechanical properties in a hot-rolled dual phase steel with different transformation temperatures were investigated in this paper. The deformation behavior of bainite and ferrite was analyzed by using in situ scanning electron microscope. The results showed that the ferrite and bainite can be refined and the volume fraction of bainite can be slightly increased by 5% by decreasing the ferrite transformation temperature from 690 to 635 °C and increasing the bainite transformation temperature from 400 to 450 °C. The strengthening mechanism was dislocation difference in polygonal and acicular ferrite and then the grain size difference of ferrite. The hole expansion ratio increased from 52.9 to 83.7% with the ferrite transformation temperature decreasing. The cracks or voids were smaller in size and also the number in steel with the lower ferrite transformation temperature after expanding. The microstructure separation along the boundary between bainite and ferrite and the slip band in the ferrite appeared at the non-uniform deformation stage. However, fewer appeared in the microstructure of steel with lower ferrite transformation temperature. Cooperative deformation of ferrite and bainite and finer microstructure in steel with lower ferrite transformation temperature were the mechanisms why the cracks could not easily nucleated and propagated, respectively. Thus this was also why there was a better hole expansion ratio.

Keywords Dual phase steel · Transformation temperature · Microstructure · Mechanical properties · Hole expansion ratio

1 Introduction

Hot-rolled dual phase steel has been one of the most common used advanced high strength steel for its high strength, low yield ratio, high initial work hardening rate and good combination of strength, plasticity and toughness [1, 2]. For

✉ Bo Jiang
  jiangbo@ustb.edu.cn

✉ Yazheng Liu
  lyzh@ustb.edu.cn

1 School of Materials Science and Engineering, University of Science and Technology Beijing, Beijing 100083, China

2 Technology Center, Maanshan Iron and Steel Co., Ltd., Maanshan 243002, Anhui, China

3 Science and Technology Development and Innovation Center, Beijing Research Institute of Mechanical and Electrical Technology, Beijing 100083, China

4 Qinghai Special Steel Engineering Technology Research Center, Xining Special Steel Co. Ltd., Xining 810005, Qinghai, China

the dual phase steel sheets used on some automotive parts, such as wheels, chassis and so on, particular elongation and stretch-flangeability are required to have higher press formability [3, 4]. The hole expansion ratio is a very important sheet formability index to describe the stretch-flangeability of sheet steel [3, 5]. Most literatures in the past [6–8] have focused on the mechanical properties and microstructures of ferrite-martensite dual phase steel because of its high strength and good ductility. However, compared with ferrite-martensite dual steels, the ferrite–bainite dual steels now have been more and more focused on the automotive materials because they have high hole expansion ratio, good strength and elongation together [2, 4, 9, 10].

There have been some reports investigating the microstructure and property of ferrite–bainite dual steels by controlled rolling and cooling or alloying methods in order to achieve a better comprehensive mechanical properties [2, 11–14]. Kumar's et al. [2] investigation presented the structure–property relations of a series of low carbon ferrite–bainite dual phase microstructures containing 50%–90% bainite prepared by varying the heat treatment of

a Nb-bearing steel. The results showed that ferrite–bainite dual phase steel with 60%–70% bainite appears to possess excellent mechanical properties such as hardness, yield and tensile strength, percentage elongation and strain-hardening exponent [2]. Shen et al. [12] investigated the effects of coiling temperature on microstructure and mechanical properties of a ferrite–bainite dual phase steel and showed that the volume fraction and the grain size of ferrite were almost independent of the coiling temperature. They concluded that lowering coiling temperature led to the hard phase changing from bainite to martensite and thus the deformation compatibility was weakened and the hole expansion ratio was reduced. Cho et al. [9] focused on the cooling condition on the microstructure and mechanical properties of Nb-bearing TS 590 MPa grade hot-rolled high strength steels. They reported that elongation and stretch-flangeability of the ferrite–bainite steel could be improved as compared with that of ferrite-pearlite steel because the formation and propagation of micro-cracks were suppressed during deformation. Most of previous studies [9, 12–16] researched on the hole expansion ratio differences of different hard phases or different volume fraction of hard phases in a dual phase steel. They showed the morphologies near the fracture surface of the specimens after expanding and discussed the propagation of micro-cracks or voids. However, few has showed the hole expansion ratio differences of steel with nearly the same hard phase but the different grain size. Also, to the best of my knowledge, nobody has shown how and why the nucleation of micro-cracks was different during expanding by in situ observing the evolution of ferrite and bainite quantificationally.

In this paper, the effect of transformation temperatures of ferrite and bainite on the microstructure and mechanical properties of ferrite–bainite dual phase were studied. The effect of microstructures on the hole expansion ratio were also discussed. In situ SEM observation of the morphologies evolution of ferrite and bainte during deformation were shown to analyze the deformation behavior and thus to explain how and why the nucleation of micro-cracks were different in different microstructures.

2 Experimental Section

2.1 Materials and Processes

The experimental steel was produced as a rectangular billet with the length of 300 mm, the width of 200 mm and the thickness of 50 mm in a steel mill. It was then reheated, roughing rolled and finishing rolled and cooled with different processing parameters as shown in Fig. 1. The thickness of the final product was 2.6 mm. The chemical composition of the investigated steel was determined as
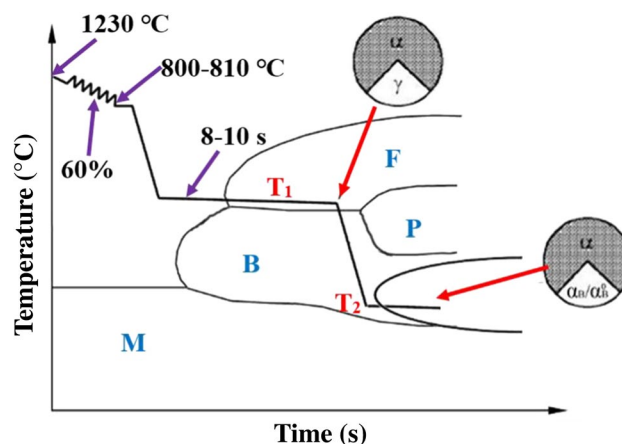

Fig. 1 The schematic route of rolling and cooling process in steel mill

0.064C–0.023Si–1.25Mn–0.016Cr and was Fe balanced. It can be seen in Fig. 1 that the cooling process of the slab after finishing rolling in the temperature range from 800 to 810 °C can be divided into several parts. At first, the slab was rapidly cooled to the temperature of T_1. After that, the slab was air cooled for 8.0–10.0 s and then coiled with the temperature of T_2. The cooling strategy was designed based on the knowledge that the ferrite transformation was in the temperature range of T_1 and the bainite transformation occurred in the temperature range of T_2. Thus, the obtained microstructure would be a mixed microstructure of ferrite and bainite. The size, the distribution and the morphology of different microstructures varied with different cooling strategies. Two cooling strategies were set in order to analyze the effect of transformation temperature and the deformation behavior. For strategy No.1, the temperatures T_1 and T_2 were set as 690 °C and 400 °C, respectively. For strategy No.2, the temperatures T_1 and T_2 were set as 635 °C and 450 °C, respectively. Metallographic examination was conducted on the center of the specimens in different directions. The samples were then mechanically ground, polished and then etched in 4% nital. Micrographs were obtained by optical microscopy (OM) (model: Scope A1).

2.2 Properties Tests and Microstructural Investigation

The mechanical properties at transverse and rolling directions of the slabs were tested. The tensile test machine CMT4105 was adopted to do the uniaxial tensile test at ambient temperature according to GB/T 228-2002 standard. Specimens for the tensile tests with 50 mm gauge length, 12.5 mm width and 2.6 mm thickness were machined from the slabs. The tensile velocity was 7.5 mm/min before yielding and 20 mm/min after yielding. In addition, the sheet formability test machine BCS-50A was

also employed to test the hole expansion performance of experimental samples at ambient temperature. The size of the square experimental slab was 100 mm × 100 mm. A hole with the diameter of 10 mm in the center of the square sample was made by punching. The punching clearance was 0.1 mm. The hole expansion test was conducted by expanding the 10 mm punched hole using a conical punch with a cone angle of 60°. The initial diameter of the hole in the sample was measured by averaging two readings taken perpendicularly to each other. When a tear at the edge of the expanding hole of the test sample was observed, the travel of the punch was stopped immediately [17]. The diameter of the expanded hole was also measured. Then, the hole expansion ratio can be expressed as follows:

$$\lambda = \frac{d - d_0}{d_0} \times 100\% \tag{1}$$

where d_0 was the average initial diameter of the hole and d the average diameter of the expanded hole. After hole expansion test, a square sample with the size of 20 mm × 20 mm was cut near the expanded hole as show in Fig. 2. The microstructures at different surfaces were observed by SEM (FEI quanta 450) to analyze the morphologies of ferrite and bainite after expanded.

In addition, in situ SEM was also employed to further analyze the morphology changes of microstructures during expanding and the deformation behavior of each phase. The previous report showed that the probability for the occurrence of a macro-crack at some sites in the region of a hole edge is much higher than at other sites. Also, they found that the strain state at those sites was similar to the strain state that occurred during uniaxial tension [3]. Consequently, it was reasonable to describe the hole expansion process by in situ tensile test. The specimens were manufactured according to Fig. 3, which is the schematic drawing of a specimen for in situ SEM tensile testing, with
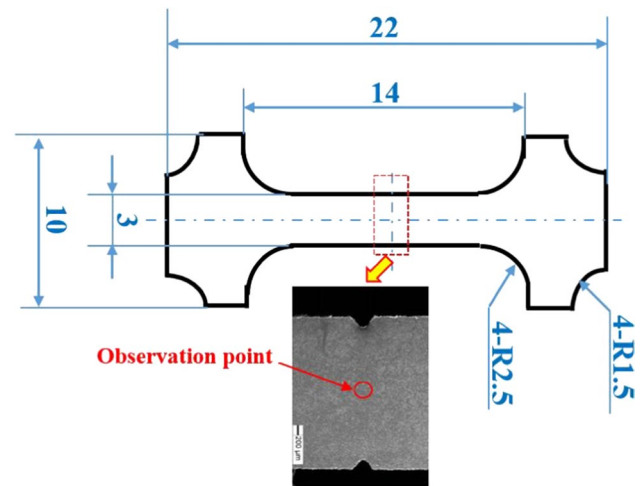

Fig. 3 The schematic drawing of a specimen for in situ SEM tensile testing (unit: mm)

thickness of 1 mm. The specimens were also machined with V shaped notch with the depth of 1 mm. Each specimen was polished and etched with 4% nital before in situ SEM investigation and testing. Specimens were then put into in situ SEM tensile test apparatus CS3400 with the maximum load of 5 kN. The tensile velocity was constant as 0.2 mm/min. All samples were tested at room temperature. The microstructures of the samples as shown in Fig. 3 were observed at different tensile deformation stages.

3 Results and Discussions

3.1 OM Microstructure

The microstructures of the investigated steel under different strategies were shown in Fig. 4. Figure 4a, b showed that the microstructures of steel along different directions under

Fig. 2 The schematic diagram of hot expansion test and the sampling position
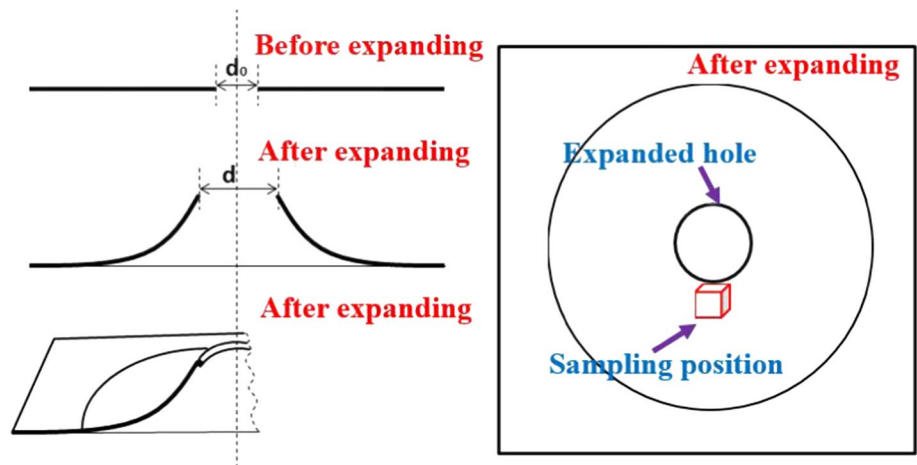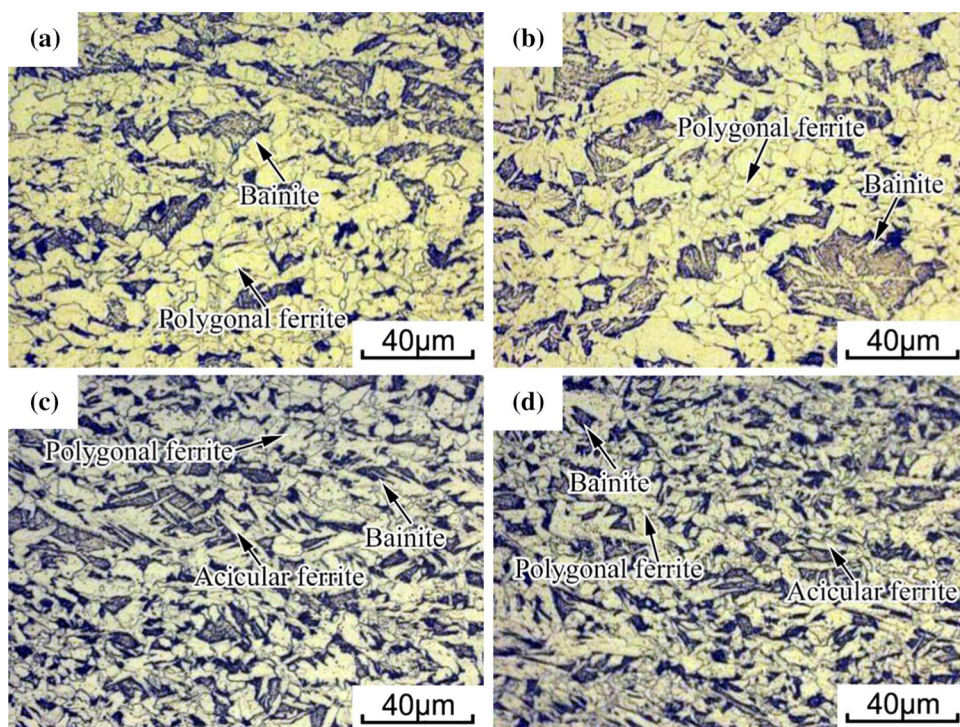
Fig. 4 Optical microstructures of steel under different strategies: strategy No.1 **a** rolling direction (RD), **b** transverse direction (TD); strategy No.2 **a** rolling direction (RD), **b** transverse direction (TD)

strategy No.1 both mainly consisted of polygonal ferrite and blocky bainite. There was no much differences of the microstructures in different directions. The size of the blocky bainite was much larger and the distribution of the bainite was also not quite uniform. The volume fraction of bainite was 19%. The average grain size of the ferrite was measured as 6.4 μm. Figure 4c, d showed that the microstructures of steel along different directions under strategy No.2 were a mixture of tiny ferrite and bainite. The ferrite and bainite could be polygonal or acicular and were dispersedly distributed. The volume fraction of bainite of steel under strategy No.2 was nearly the same but 5% more than that under strategy No.1. The results were not in accordance with the previous study which showed that bainite volume fraction increased as the coiling temperature decreased [9]. Thus, the slight increase of bainite volume fraction could be attributed to the grain refinement. The average grain size of the ferrite was measured as 5.6 μm. Ferrite formed at the temperature of 635 °C were finer than that of 690 °C. More grain boundaries of ferrite were offered for promoting the nucleation of bainite in the finer microstructure. Also, the ferrite also began to change from polygonal ferrite to acicular ferrite. Thus, the bainite was also refined and uniformly distributed because of the refinement of ferrite.

3.2 Effect of Microstructure on the Mechanical Properties and the Hole Expansion Ratio

The tensile strength, yield strength and elongation of steels at different directions under different strategies were shown

in Fig. 5a. It can be seen that the strengths at transverse direction were a little higher than that at rolling direction while the elongations were nearly the same. Comparing the mechanical properties of different strategies, the conclusion can be made that the elongation of steel under strategy No.2 was nearly the same as that of strategy No.1 though the tensile strength and yield strength of steel under strategy No.2 were much higher. The experimental results of the hot expansion test in Fig. 5b showed that there was a dramatic increase in the hole expansion ratio value of steel under strategy No.2 compared with that of strategy No.1. The average value was increased from 52.9 to 83.7%. The yield strength of ferrite σ_α can be identified as the follows [18]:

$$\sigma_\alpha = \sigma_0 + 17.4d^{-1/2} \tag{2}$$

where d is the average grain size of ferrite. It can be concluded that the yield strength difference of the ferrite σ_α in steels under two different strategies contributed by the grain size difference was 15 MPa. However, the total difference of yield strength in average was nearly 45 MPa. The strength of bainite transformed at higher temperature was higher because of the difference in dislocation density. Thus, the yield strength difference of bainite in steels under different strategies can be nearly neglected because the volume fraction of bainite was only 5% more but the transformation temperature of bainite was 50 °C higher in steel under strategy No.2. In conclusion, the strengthening mechanism of steel under strategy No.2 could be attributed to dislocation difference in polygonal and acicular ferrite and then
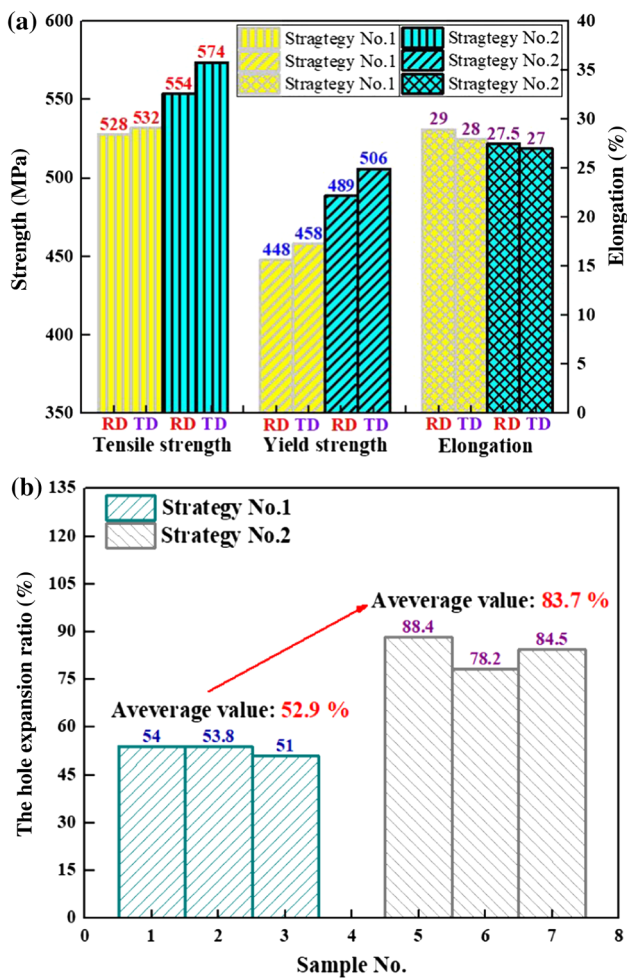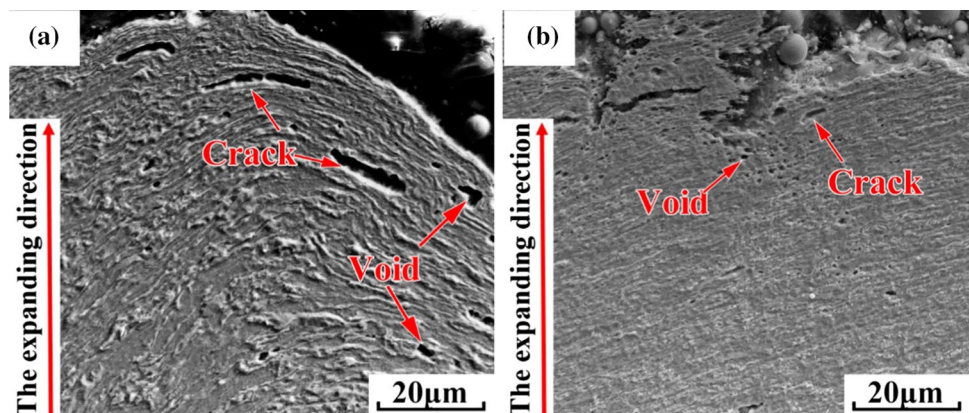
(a)

(b)

Fig. 5 **a** Mechanical properties and **b** hole expansion ratio of steels under different strategies

the grain size difference of ferrite. The former one was the main point. Also it was not surprising that the refinement of microstructure had not damaged the elongation when the strength was increased. The results were unanimous to many

previous reports [19–21]. However, the hole expansion ratio was greatly improved when the microstructure was changed.

The microstructure was observed by SEM to further analyze the microstructure effect during hot expansion test. Figure 6 showed the microstructures of steel along the expanding direction after the hole expansion test. It can be seen in the figure that there were cracks and voids near the final fracture surfaces. The cracks and voids in the steel under strategy No.1 were mainly formed along the boundaries of large polygonal ferrite or the boundaries between ferrite and bainite. The results were ananimous to the previous reports [9, 12, 16]. However, the cracks or voids in the steel under strategy No.2 were smaller in size and also the number. During the expanding deformation process, the voids or small cracks can often be formed at the boundary or inclusions at the first stage because of the stress concentration. The stress concentration often occurred at the boundaries between ferrite and bainite due to the difference of deformation ability or at the ferrite boundaries. Cooperative deformation of different phases or grains could release the stress concentration and thus delay the nucleation of voids or small cracks [12]. After the nucleation of micro-cracks and voids, the cracks will propagate along the grain boundary. In the finer microstructure, the cracks grew slowly along the boundary and sometimes could even only propagate across the bainite or ferrite. Surely it would take more energy. Consequently, the hole in the specimen of strategy No.2 with finer microstructures could expand to a larger size without cracks.

3.3 Effect of Microstructure on the Deformation Behavior

In situ SEM results was employed to further analyze the morphology changes of microstructures before crack formation during expanding. The stress-distance curves of in situ SEM tensile test of steel under different strategies were shown in Fig. 7. It can be seen that the tensile process could be divided into three stages: uniform deformation stage, non-uniform deformation stage and crack formation stage. It was obvious

Fig. 6 SEM microstructures of steel after the hole expansion test: **a** strategy No.1, **b** strategy No.2

that steel under strategy No.2 has a longer uniform deformation stage. The typical microstructures at different positions as marked at the curves were shown in Figs. 8 and 9. It can be seen that the bainite and ferrite in the microstructures were elongated with tensile process. The lengths of bainite and ferrite at different tensile stages were measured in order to analyze the deformation behavior. The length of bainite was marked as L_B and that of ferrite was L_F as shown in Fig. 8a. The length of each phase increased with the tensile process. The elongation of different phases at a point was set as A which can be expressed as follows:

$$A = \frac{L' - L_a}{L_a} \times 100\% \tag{3}$$

where L' was the length of the phase at the point of the tensile process; L_a was the length of the phase at the starting point a of the tensile process. The coefficient K of different phases were calculated based on Eq. 4 to analyze the effect of elongation change of the specimen on the elongation change of each phase during tensile process. It was defined as the follows:

$$K = \frac{\Delta A}{\Delta A_S} \times 100\% \tag{4}$$

where ΔA at a point was the difference value of the elongation A at this point and the elongation at the former point; ΔA_S at a point was the difference value of the elongation of the specimen A_S at this point and the elongation of the specimen at the former point. Three points were measured and the corresponding K values were calculated in each steel and they showed the same trend. The typical calculated K values of different phases in steel under different strategies have been shown in Fig. 10.

The results showed that the K values of ferrite and bainite were nearly the same at the uniform deformation stage as shown in Fig. 10 which indicated that the ferrite and bainite deformed coordinately. The K value of ferrite was smaller than that of bainite in this stage due to the higher deformation ability of ferrite. However, the K value of each phase increased sharply when the non-uniform deformation began. The non-uniform deformation of steel under strategy No.2 began after point f while that of strategy No.1 began much earlier. The microstructure separation along the boundary between bainite and ferrite and the slip band in the ferrite began to appear in the microstructure as shown Figs. 8e, f and 9g. However, fewer appeared in the microstructure of steel with lower ferrite transformationtemperature. The microstructure separation along the boundary and the slip band in the ferrite could be the sites of stress concentration and the nucleation of cracks. The K value of each phase in

Fig. 7 The stress-distance curves of in situ SEM tensile test of steel under different strategies: **a** strategy No.1, **b** strategy No.2
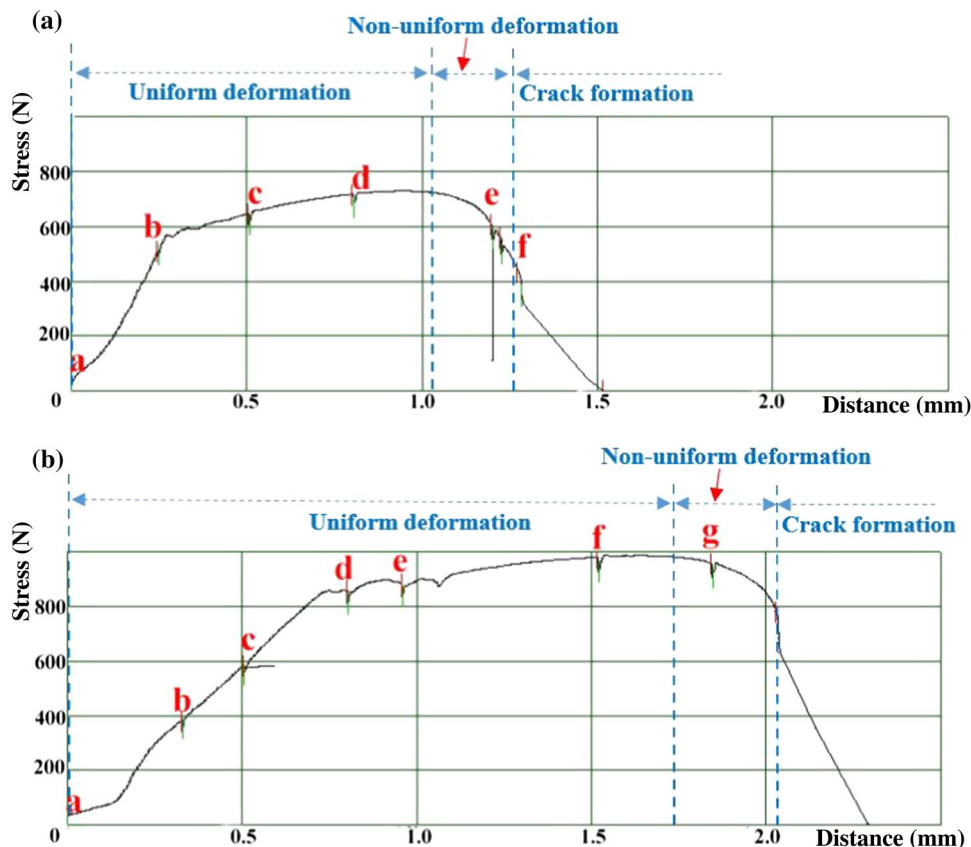
Fig. 8 In situ SEM micro-structures at different tensile positions of the stress-distance curve of steel under strategy No.1 as shown in Fig. 7a: **a** a, **c** c, **e** e, **f** f
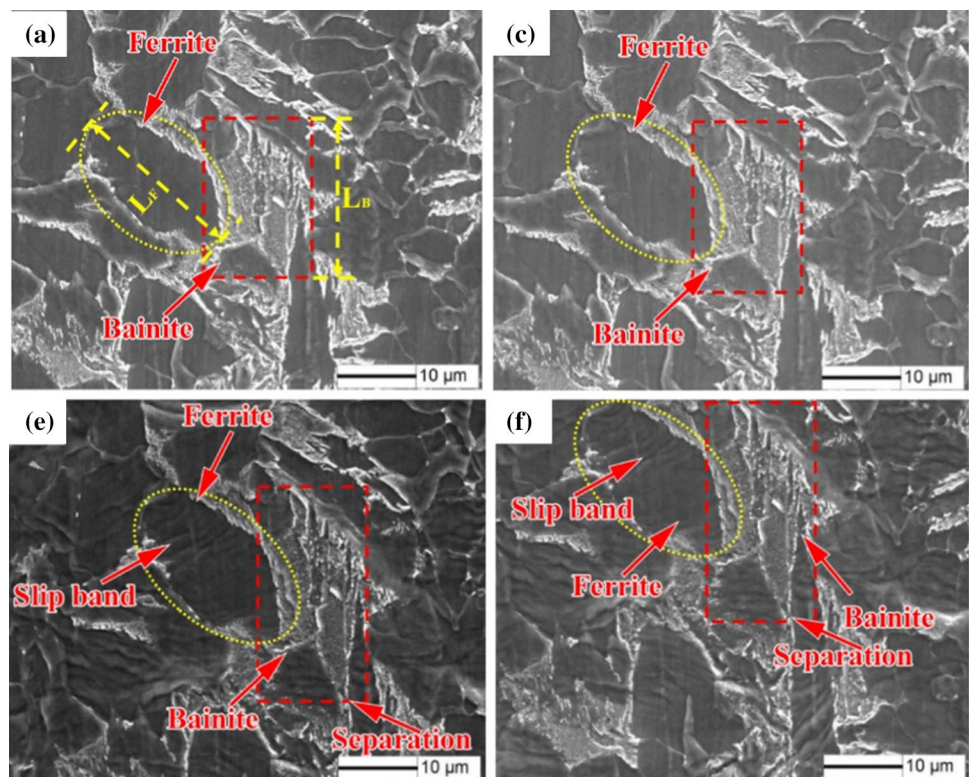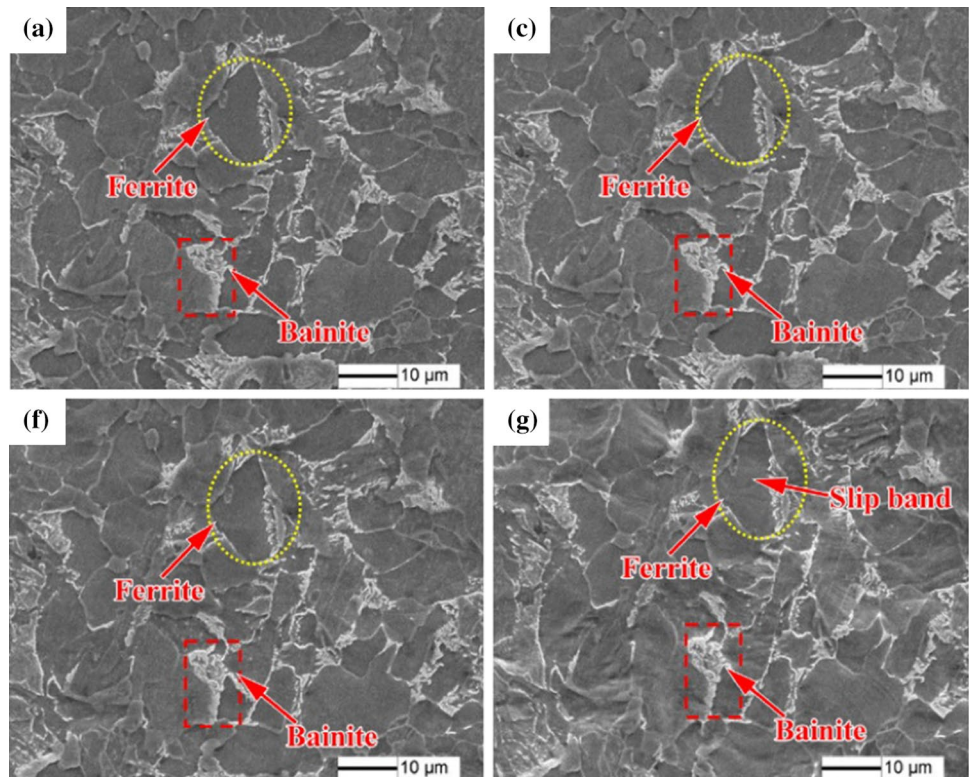

Fig. 9 In situ SEM micro-structures at different tensile positions of the stress-distance curve of steel under strategy No.2 as shown in Fig. 7b: **a** a, **c** c, **f** f, **g** g

steel strategy No.1 was also quite higher than that of strategy No.2. This indicated that the ferrite and bainite in steel under strategy No.1 deformed more dramatically. At the non-uniform deformation stage, the difference value of K between ferrite and bainite also began to increase. In Fig. 10, it was shown that the difference value of K reached 8 at
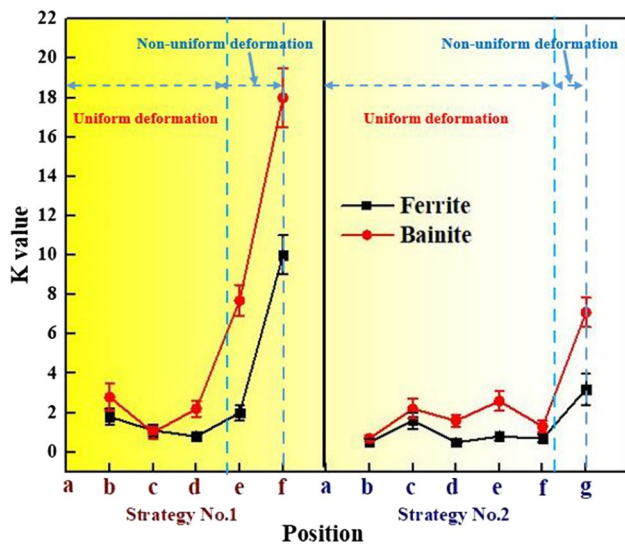
Fig. 10 The coefficient *K* of different phases in steel under different strategies

point f in steel under strategy No.1. However, the difference value of *K* was quite lower and only nearly 4 at point g in steel under strategy No.2 as shown in Fig. 10. In the steel under strategy No.2, the ferrite and bainite could still deform relatively more coordinately even at the non-uniform deformation stage. This is why the stress concentration could be improved and the cracks could not easily nucleated, and thus there was a better hole expansion ratio in the steel under strategy No.2.

4 Conclusions

1. The ferrite and bainite can be refined and the volume fraction of bainite can be slightly increased by 5% by decreasing the ferrite transformation temperature from 690 to 635 °C and increasing the bainite transformation temperature from 400 to 450 °C. Also, the ferrite began to change from polygonal ferrite to acicular ferrite and the microstructure was distributed more dispersedly due to the refinement of ferrite.

2. The strength of steel with the ferrite transformation temperature of 635 °C was higher than that of 690 °C. The strengthening mechanism was dislocation difference in polygonal and acicular ferrite and then the grain size difference of ferrite. The hole expansion ratio increased from 52.9 to 83.7% with the ferrite transformation temperature decreasing. The cracks or voids were smaller in size and also the number in the samples with lower ferrite transformation temperature after expanding.

3. The *K* value of each phase increased sharply when the non-uniform deformation began. The steel with lower

ferrite transformation temperature has a longer uniform deformation stage. The ferrite and bainite steel with higher ferrite transformation temperature deformed more dramatically at the non-uniform deformation stage. The microstructure separation along the boundary between bainite and ferrite and the slip band in the ferrite appeared at the non-uniform deformation stage. However, fewer appeared in the microstructure of steel with lower ferrite transformation temperature.

4. The difference value of *K* between ferrite and bainite in the steel with lower ferrite transformation temperature was quite lower than that of higher ferrite transformation temperature. The ferrite and bainite in steel with lower ferrite transformation temperature could still deform relatively more coordinately even at the non-uniform deformation stage. Cooperative deformation of ferrite and bainite and finer microstructure in steel with lower ferrite transformation temperature were the mechanisms why the cracks could not easily nucleated and propagated, respectively. Thus this was also why there was a better hole expansion ratio.

References

1. Y.L. Kang, Lightweight vehicle, advanced high strength steel and energy-saving and emission reduction. Iron Steel **43**(6), 1–7 (2008) **(in chinese)**

2. A. Kumar, S.B. Singh, K.K. Ray, Influence of bainite/martensite-content on the tensile properties of low carbon dual-phase steels. Mater. Sci. Eng. A **474**(1–2), 270–282 (2008)

3. S.H. Choi, E.Y. Kim, S.I. Kim, The micromechanical deformation behaviors of hot-rolled 590FB steel during hole-expansion test. Int. J. Plast **58**, 184–200 (2014)

4. S. Hashimoto, M. Sudo, K. Mimura et al., Effect of microstructure on mechanical properties of C-Mn high strength hot rolled sheet steel. Trans. Iron Steel Inst. Jpn. **26**(11), 985–992 (1986)

5. J. Lee, S.J. Lee, B.C. De Cooman, Effect of micro-alloying elements on the stretch-flangeability of dual phase steel. Mater. Sci. Eng. A **536**, 231–238 (2012)

6. A. Kamp, S. Celotto, D.N. Hanlon, Effects of tempering on the mechanical properties of high strength dual-phase steels. Mater. Sci. Eng. A **538**, 35–41 (2012)

7. I. Pushkareva, S. Allain, C. Scott et al., Relationship between microstructure, mechanical properties and damage mechanisms in high martensite fraction dual phase steels, in *ISIJ International. ISIJINT-2015-186* (2015)

8. J.I. Yoon, J. Jung, H.H. Lee et al., Relationships between stretch-flangeability and microstructure-mechanical properties in ultra-high-strength dual-phase steels. Met. Mater. Int. (2019). https://doi.org/10.1007/s12540-019-00270-x

9. Y.R. Cho, J.H. Chung, H.H. Ku et al., Effect of controlled cooling on the formability of TS 590 MPa grade hot-rolled high strength steels. Met. Mater. **5**(6), 571–578 (1999)

10. D.I. Hyun, S.M. Oak, S.S. Kang et al., Estimation of hole flangeability for high strength steel plates. J. Mater. Process. Technol. **130**, 9–13 (2002)
11. J. Lee, S.J. Lee, B.C. De Cooman, Effect of micro-alloying elements on the stretch-flangeability of dual phase steel. Mater. Sci. Eng. A **536**, 231–238 (2012)
12. X.J. Shen, X.H. Pei, S. Tang et al., Effects of coiling temperature on microstructure and mechanical properties of hot-rolled ferrite/bainite dual phase steel. J. Northeast. Univ. (Nat. Sci.) **35**(8), 1120–1123 (2014) **(in chinese)**
13. W.W. Wang, H. Ding, Z.Y. Tang et al., Stretch-flangeability of ferrite–bainite steel. J. Iron Steel Res. **21**(6), 48–52 (2009) **(in chinese)**
14. X. Fang, Z. Fan, B. Ralph et al., The relationships between tensile properties and hole expansion property of C-Mn steels. J. Mater. Sci. **38**(18), 3877–3882 (2003)
15. A. Kaijalainen, V. Kesti, R. Vierelä et al., The effect of microstructure on the sheared edge quality and hole expansion ratio of hot-rolled 700 MPa steel. J. Phys. Conf. Ser. **896**(1), 012103 (2017)
16. M. Cai, H. Ding, Y. Lee et al., Effects of Si on microstructural evolution and mechanical properties of hot-rolled ferrite and bainite dual-phase steels. ISIJ Int. **51**(3), 476–481 (2011)
17. X. Fang, Z. Fan, B. Ralph et al., Effects of tempering temperature on tensile and hole expansion properties of a C-Mn steel. J. Mater. Process. Technol. **132**(1–3), 215–218 (2003)
18. B.C. De Cooman, J.G. Speer, *Fundamentals of Steel Product Physical Metallurgy* (AIST, Association for Iron & Steel Technology, Warrendale, 2011)
19. Q. Yong, *Second Phases in Structural Steels* (Metallurgical Industry Press, Beijing, 2006)
20. G. Dini, A. Najafizadeh, R. Ueji et al., Tensile deformation behavior of high manganese austenitic steel: the role of grain size. Mater. Des. **31**(7), 3395–3402 (2010)
21. G. Jha, S. Das, S. Sinha et al., Design and development of precipitate strengthened advanced high strength steel for automotive application. Mater. Sci. Eng. A **561**, 394–402 (2013)